Med Chem Res (2010) 19:629–642
DOI 10.1007/s00044-009-9218-4

MEDICINAL CHEMISTRY RESEARCH

ORIGINAL RESEARCH

Structure-based molecular design, synthesis, and in vivo anti-inflammatory activity of pyridazinone derivatives as nonclassic COX-2 inhibitors

Khaled A. M. Abouzid · Nadia A. Khalil · Eman M. Ahmed · Hekmat A. Abd El-Latif · Moustafa E. El-Araby

Received: 28 January 2009 / Accepted: 17 April 2009 / Published online: 27 May 2009

Abstract A scaffold with bicyclic core carrying pyridazinone moiety, which exhibited potent in vivo anti-inflammatory activities, was introduced in this article. The design of these compounds was assisted by docking and superposition experiments on cyclooxygenase-2 enzyme. The activity of a chloro analogue was as high as that of diclofenac in carrageenan-induced rat paw edema anti-inflammatory screening.

Keywords Quinoxaline · Pyridazinone · Anti-inflammatory · Molecular design · Synthesis

Introduction

There is a great deal of renewed interest in cyclooxygenase-2 (COX-2), a key inducible enzyme for the synthesis of prostaglandins, as a therapeutic target (McKellar *et al*., 2008; Jankowski and Hunt, 2008). The introduction of COX-2

K. A. M. Abouzid (✉)
Pharmaceutical Chemistry Department, Faculty of Pharmacy, Ain Shams University, Cairo 11566, Egypt
e-mail: abouzid@yahoo.com

N. A. Khalil · E. M. Ahmed
Organic Chemistry Department, Faculty of Pharmacy, Cairo University, Cairo 11562, Egypt

H. A. A. El-Latif
Pharmacology Department, Faculty of Pharmacy, Cairo University, Cairo, Egypt

M. E. El-Araby
Pharmaceutical Organic Chemistry Department, Faculty of Pharmacy, Helwan University, Helwan 11795, Egypt
e-mail: alamka@yahoo.com

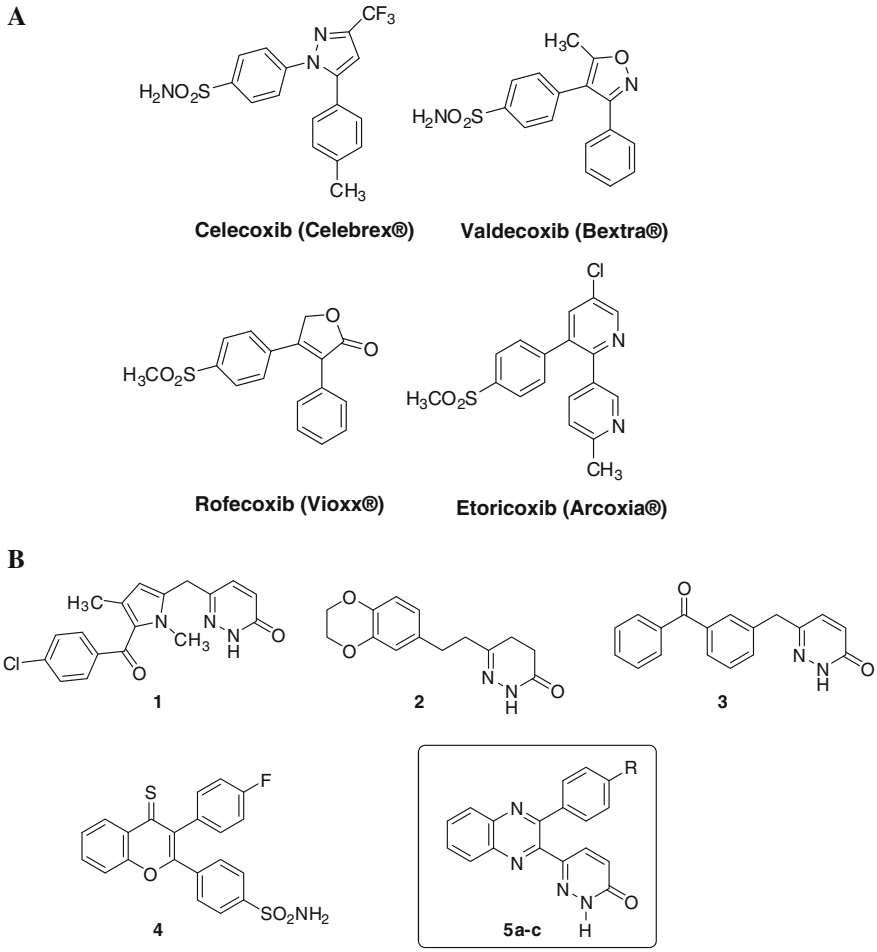

Fig. 1 Representative of potent COX-2 inhibitors: **a** Market classic COX-2 inhibitors; **b** literature pyridazinone derivatives 1–4 and our quinoxaline derivatives **5a–c**

inhibitors (coxibs), such as celecoxib, rofecoxib, and valdecoxib (Fig. 1) in the 1990s was viewed as a milestone triumph over human suffering of pain and inflammation with little or no damage to the gastric mucosa, a well-known side effect of classic nonsteroidal anti-inflammatory drugs (NSAIDs) (Flower, 2003). Unfortunately, rofecoxib (Vioxx®) was withdrawn from the market in the fall of 2004 after clinical reports of its linkage to elevated risk of cardiac stroke (Abramson and Greenberg, 2008). The only upside of the Vioxx® crisis is that no concrete evidence has been introduced to conclude that COX-2 inhibition itself is the sole factor in such cardiac problems; otherwise, there would be widespread side effects for all selective COX-2 inhibitors and, possibly, nonselective COX-1 and COX-2 inhibitors (classic NSAIDs). It was argued that these adverse actions of rofecoxib may be mediated by a maleic anhydride metabolite rather than the inhibition of

prostacyclin, a prostaglandin involved in the prevention of cardiac stroke (Reddy and Corey, 2005). Therefore, a new generation of COX-2 inhibitors that are radically different from the first-generation coxibs are anticipated to avoid the cardiac untoward effects. The second reason that spotlighted COX-2 was the discovery of its increased expression in certain types of solid tumors, such as gastric cancer (Yamac *et al*., 2008), pancreatic cancer (Tucker *et al*., 1999), esophageal cancer (Li *et al*., 2001), and colorectal cancer (Arber, 2008). Although the exact mechanism of COX-2 in carcinogenesis is not completely understood, it was suggested that it is due to up-regulation of prostaglandin-induced angiogenesis (Sinicrope and Gill, 2004).

The basic structural features of the classic COX-2 inhibitors included a central trisubstituted monocyclic planar ring (usually five-membered heterocycles) attached to two pendent benzene rings and a lipophilic group. One of the phenyl groups is attached to sulfamyl (celecoxib and valdecoxib) or methylsulfonyl (rofecoxib and etoricoxib). The sulfonated benzene moiety penetrates a narrow hydrophilic pocket, which is not accessible in COX-1, and hence, it achieves the COX-2 selectivity (Gierse *et al*., 1996). Recent reports successfully used nonclassic isosteres of the sulfonylaryl group, such as pyridazinone (compounds **1–3**) to make potent COX-2 inhibitors (Chintakunta *et al*., 2002; Li *et al*., 2003; Abouzid and Bekhit, 2008).

Other reports introduced an atypical central part, such as bicyclic rings (Ranatunge *et al*., 2004; Beswick *et al*., 2004; Whitehead *et al*., 2007), *Z*-olifens (Jashim Uddin *et al*., 2004), biphenyls (Chen *et al*., 2005), and other scaffolds (Kalgutkar and Zhao, 2001). For instance, compound **4**, a bicyclic derivative with fused six-membered rings, was found to be a potent COX-2 inhibitor in vitro but it lacked in vivo potency (Joo *et al*., 2003). In this report, we are used a combination of these two approaches to design and synthesize novel COX-2 inhibitors **5** designed to keep the potency while moving away from the classic coxib structures to reduce side effects.

Rationale and structure-based drug design

Our design is based on a two-point structural modification: 1) central bicyclic quinoxaline scaffold carrying only one phenyl ring; and 2) pyridazinone moiety as a replacement of sulfamylphenyl or sulfonylphenyl group. The benzene portion of the fused quinoxaline ring was used to cover the area occupied by the CF_3 group of celecoxib. This was confirmed by structure-based molecular modeling studies, which were performed using the SYBYL molecular modeling package. The COX-2 enzyme crystal structure coordinates were downloaded from the Protein Data Bank (PDB entry: 6COX), which contains SC-558 as selective COX-2 inhibitor in its active site (Kurumbail *et al*., 1996). SC-558 is a closely related congener to celecoxib that differs only in having bioisosteric bromo group in replacement of the *para* methyl on the pendent phenyl group.

The structure of **5a** was constructed using the BUILD/EDIT option of SYBYL using fragments, groups, and atoms from SYBYL substructure library. The structure was given Gasteiger-Marsili charges. The built structure were subjected to geometry

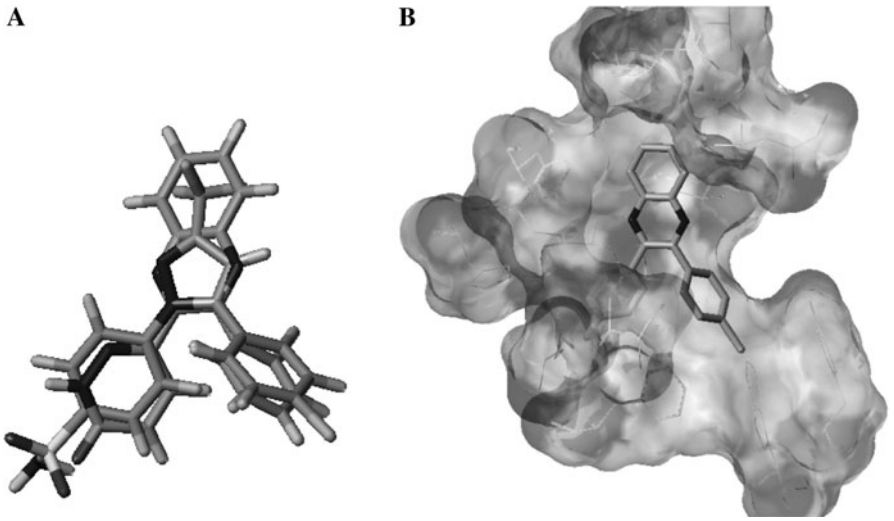

Fig. 2 **a** The pyridazine derivative **5a** superposed with SC-558. **b** The potent COX-2 inhibitor **5b** shown inside the active site (expressed by Connolly surface)

optimization by running energy minimization using the following parameters: MAXIMIN2 minimizer, gradient energy change, 0.01 kcal/Å mol; rms displacement, 0.001 Å; nonbonded cutoff, 8.000 Å; dielectric function, distant dependent; dielectric constant, 1.00; iteration: until convergence.

We performed the modeling studies in two ways. First, we tested the superposition of the designed compound **5a** with SC-558 (Fig. 2). Second, we performed docking experiments of the new quinoxaline **5** structure models on the active site of the COX-2 structure coordinates after removing SC-558. The results showed very good superposition and binding opportunity for the designed scaffold.

Chemistry

As shown in Scheme 1, the synthesis started with preparation of intermediate benzylidenelevulenic acid **6** by condensation of levulenic acid with certain aromatic aldehydes (Zaheer *et al*., 1956; Sircar *et al*., 1989). Cyclization of **6** with hydrazine hydrate afforded the corresponding intermediate 4,5-dihydropyridazinones **7** according to the reported method (Sircar *et al*., 1989; Baddar *et al*., 1972). Bromination of **7** followed by a second cyclization using *o*-phenylenediamine afforded the partially saturated congeners **9**, which were again treated with bromine and acetic acid to furnish the target compounds **5a–c** (Coudert *et al*., 1988).

Attempts for cyclization of **8** with ethylenediamine resulted in dehydrobromination and the formation of **10** (Scheme 2). Apparently, ethylenediamine behaved as a base rather than a nucleophile in this reaction.

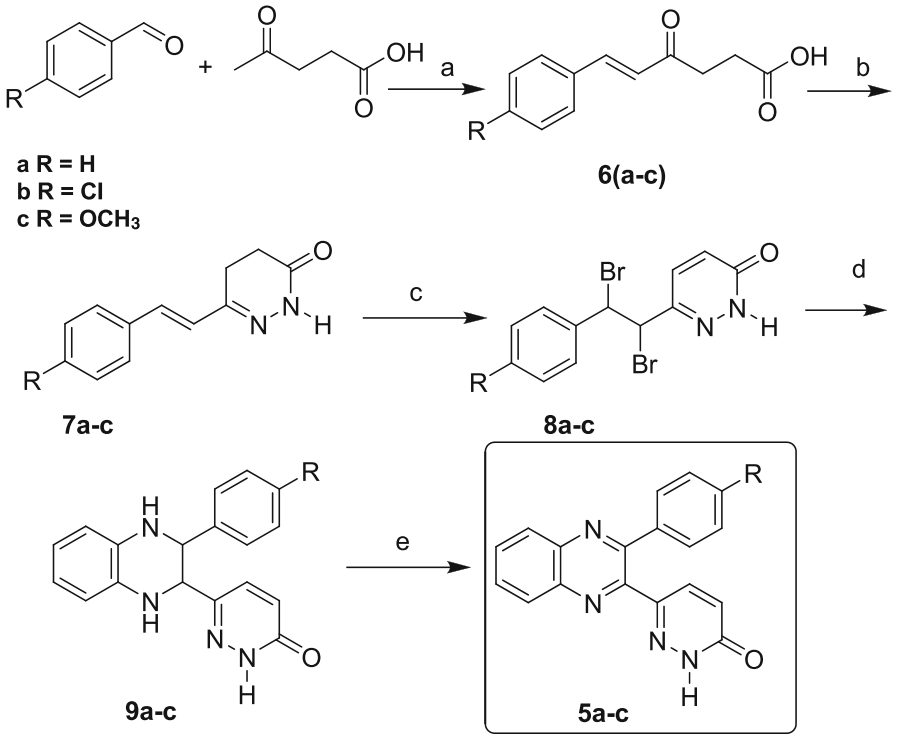

Scheme 1 Reagents: **a** morpholine, AcOH, C_6H_6, heat; **b** $NH_2NH_2.H_2O$, AcOH; **c** Br_2 (2 equiv.), AcOH; **d** *o*-phenylenediamine, Et_3 N, EtOH, heat; **e** Br_2 (2 equiv.), AcOH

In vivo anti-inflammatory screening

The in vivo anti-inflammatory effect of quinoxaline derivatives **5a–c** and **9a–c** was evaluated using Paw Volume method in carrageenan-induced rat paw edema model (see experimental section for method details) (DiRosa and Willoughby, 1971). The results of edema reduction are presented in Table 1 and Fig. 3.

Results and discussion

The quinoxaline scaffold represented by the compound **5a** showed activity in both docking model and in anti-inflammatory activity test compared with diclofenac (Fig. 3). The two aryl groups are pointing to the same area of space; nevertheless, the question was about opportunities and mode of binding of pyridazinone ring. As shown in Fig. 2, Docking of **5a** on the active site of COX-2 crystal structure produced a complex with total energy comparable to the original crystal structure. The compound **5a** is situated in the active site without unfavorable interactions by visual inspections as well as by docking energies (Fig. 2b).

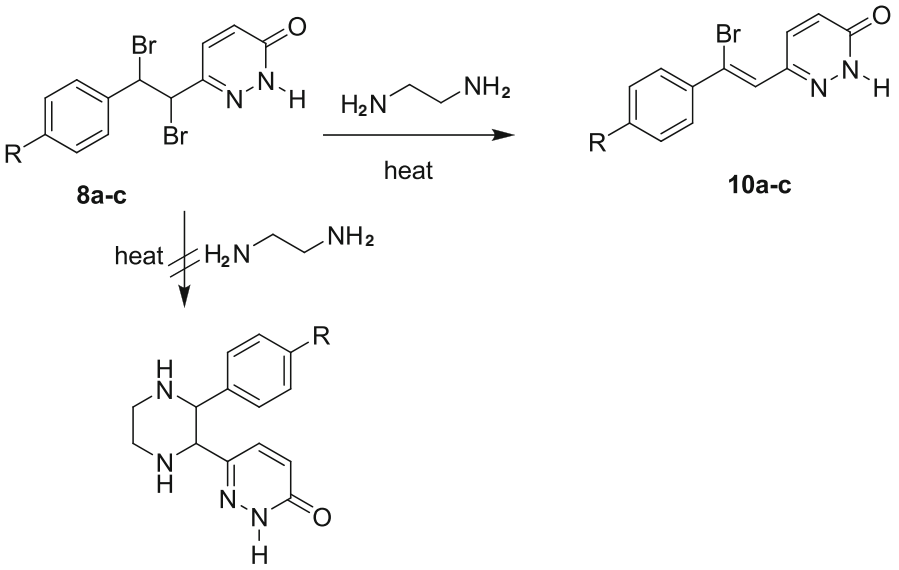

Scheme 2

Table 1 Inhibition of rat paw edema compared with the control at different time intervals after treatment with a single dose (5 mg/kg) of diclofenac or test compounds

Compound	Time intervals (hr)				
	After injection	1	2	3	4
Control	1.95 ± 0.03[a]	1.95 ± 0.03[c]	2.00 ± 0.03[d]	2.03 ± 0.02[e]	2.20 ± 0.04[d]
5a	2.00 ± 0.00[a]	1.97 ± 0.02[c]	1.37 ± 0.06[c]	1.00 ± 0.07[c]	0.38 ± 0.07[b]
5b	1.97 ± 0.02[a]	1.48 ± 0.03[b]	0.95 ± 0.04[b]	0.55 ± 0.04[b]	0.03 ± 0.02[a]
5c	1.97 ± 0.02[a]	1.55 ± 0.09[b]	1.50 ± 0.10[c]	1.38 ± 0.06[d]	1.27 ± 0.08[c]
9a	2.00 ± 0.00[a]	2.00 ± 0.00[c]	2.02 ± 0.02[d]	2.00 ± 0.00[e]	2.07 ± 0.03[d]
9b	1.95 ± 0.02[a]	1.93 ± 0.03[c]	1.93 ± 0.03[d]	2.00 ± 0.04[e]	2.12 ± 0.05[d]
9c	2.00 ± 0.00[a]	1.58 ± 0.09[b]	1.42 ± 0.04[c]	1.38 ± 0.05[d]	1.32 ± 0.06[c]
Diclofenac	1.97 ± 0.02[a]	0.92 ± 0.03[a]	0.57 ± 0.03[a]	0.3 ± 0.03[a]	0.03 ± 0.02[a]
F value	0.88	50.20	102.87	234.20	321.97
P value	0.534	0.000*	0.000*	0.000*	0.000*

All values are represented as mean ± standard error. a, b, and c = results with same letter has no significant difference by using Turkey HSD multiple comparison test at $P < 0.06$

The top of the active site gorge is occupied by the fused benzene ring, and the pendent phenyl fits in the main hydrophobic channel of the active site. The pyridazinone moiety is placed inside the hydrophobic pocket, which determines the most selectivity of COX-2 inhibitors over COX-1 (Gierse *et al.*, 1996). As seen Fig. 4, there are effective hydrogen bonding network between the pyridazinone and

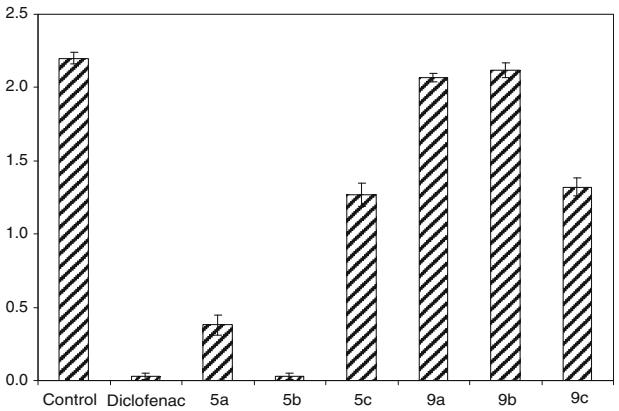

Fig. 3 Effect of test compounds on carrageenan-induced inflammation in rats after 4 h

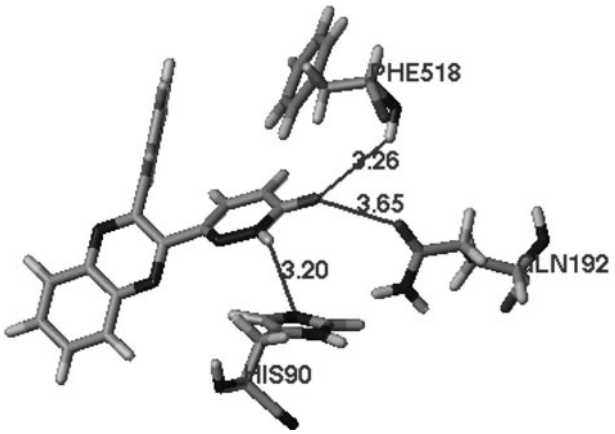

Fig. 4 Image of docking of **5a** on the active site to illustrate interactions of the pyridazine moiety with residues in the hydrophilic side pocket. Numbers indicate H-Bond distances

His-90, Gln-192, and Phe-518 (main chain NH) (Kurumbail *et al*., 1996; Slater *et al*., 2001). Due to dissimilarity of the two sides of the pyridazine ring, docking experiments investigated the possibility of flipping of the heterocyclic ring inside the hydrophilic channel. It was found that this situation results in poor docking model because the polar side is interacting with the lipophilic phenyl group of Phe-518 and some other nonpolar residues while the carbocyclic side loses hydrogen-bonding contacts. As expected, the pendent phenyl group is properly filling the main hydrophobic channel of the active site. This pocket is surrounded by a group of aromatic and aliphatic nonpolar amino acid side chains, such as Val-528, Tyr-385, Trp-387, Phe-518, and Leu-352. Note that the last two residues are interacting with the nonpolar (carbocyclic) side of the pyridazinone ring (Fig. 5a).

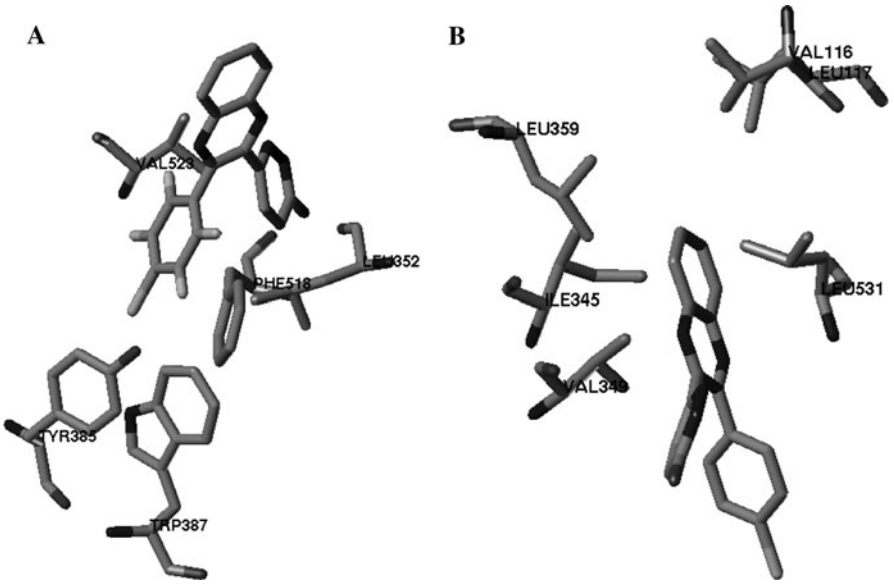

Fig. 5 Docking of the chloro compound **5b** on the active site: **a** Interactions of *p*-chlorophenol moiety with residues of some active site's hydrophobic gorge; **b** interaction of the bicyclic quinoxaline moiety with other hydrophobic residues

Regarding substituents on the pendent phenyl group, the model predicted that bulky or polar groups are not desired on the pendent phenyl ring due to limitation in pocket size and the lipophilic nature of the surrounding residues (Figs. 2 and 5b). This might explains the poor activity of the methoxy analogue **5c** in pharmacological screening. In contrast, the model predicted high potency of the chloro analogue **5b** as the chloro group interacts properly with the aromatic ring of Tyr-385.

Our study confirmed the importance of the planar aromatic nature of the central scaffold, a SAR feature that is not frequently discussed in COX-2 inhibitors (Kalgutkar and Zhao, 2001; Garg *et al*., 2003). Loss of the planarity in the nonaromatic analogue **9b** resulted in complete loss of activity. Docking of trans diastereomers of **9a** produced very poor binding as compound did not fit with active site and collided with residues surrounding it (data not shown).

Conclusions

Bicyclic quinoxaline nucleus attached to pyridazinone and phenyl substituents formed potent anti-inflammatory novel structures especially the chloro analogue **5b**. The in vivo high potency of **5b** is comparable to that of diclofenac. This combination constitutes an important development of the nonclassic bicyclic COX-2 inhibitors because it is a novel bicyclic nonsulfonated compound with high in vivo anti-inflammatory activity. The structure-based molecular design accurately

predicted the inherent activity of the scaffold and the rank of potency of the compounds **5a–c**. The study also illustrated the importance of the aromatic planar structure of the central scaffold due to the poor activity of the nonaromatic analogues **9a–c**.

Experimental

All melting points were determined on a Stuart apparatus and are uncorrected. IR spectra were determined as KBr discs on Shimadzu IR 435 spectrophotometer and values are represented in cm^{-1}. ^{1}H-NMR spectra were performed using a Varian Gemini 200 MHz spectrometer with TMS as internal standard. Chemical shift values were recorded in ppm on δ scale. Mass spectra were recorded on a Hewlett-Packard 5988 spectrometer. Elemental analyses were performed at the Microanalytical Center, Cairo University, Egypt. Progress of the reactions was monitored by TLC using TLC sheets precoated with UV florescent silica gel Merck 60 F 254 and visualized using UV light.

(E)-6-Aryl-4-oxo-5-hexenoic acids (**6a–c**) and 4,5-dihydro-3(*2H*)-pyridazinones (**7a–c**) were prepared according to reported procedures (Zaheer *et al*., 1956; Sircar *et al*., 1989).

2-Aryl-3-(6-oxo-1,6-dihydropyridazin-3-yl)quinoxaline (5a–c)

To a vigorously stirred solution of 0.01 mol of the appropriate **9a–c** (0.01 mol) in glacial acetic acid (20 ml) kept at 70–80°C, bromine (0.02 mol) was added portionwise for 15 minutes. The mixture was stirred further for 3 hours at the same temperature and poured into ice-cold water (50 ml). The separated solid was filtered, washed with water, and crystallized from ethanol to give **5a–c**.

2-Phenyl-3-(6-oxo-1,6-dihydropyridazin-3-yl)quinoxaline (5a) was obtained as white solid, yield: 70%; mp: >300°C. IR (ν, cm^{-1}): 3500–3300 (NH), 1680 (C=O). ^{1}H-NMR (DMSO-d_6) δ: 7.06 (d, $J = 9.8$ Hz, 1H, pyridazinone H-4), 7.49–7.71 (m, 9H, Ar–H), 7.96 (d, $J = 9.8$ Hz, 1H, pyridazinone H-5), 13.22 (s, 1H, NH pyridazinone, D_2O exchangeable). EIMS *m/z*: 300 (M^+, 10.00%). Anal. Calcd. for $C_{18}H_{12}N_4O$: C, 71.52; H, 4.63; N, 18.54. Found: C, 71.84; H, 4.57; N, 18.92.

2-(4-Chlorophenyl)-3-(6-oxo-1,6-dihydropyridazin-3-yl)quinoxaline (5b) was obtained as white solid, yield: 65%; mp: >300°C. IR (ν, cm^{-1}): 3500–3300 (NH), 1680 (C=O). ^{1}H-NMR (DMSO-d_6) δ: 7.16 (d, 1H, pyridazinone H-4), 7.60–7.79 (dd, 4H, Ar–H), 8.01–8.24 (m, 5H, 4Ar–H and pyridazinone H-5), 13.27(s, 1H, pyridazinone NH, D_2O exchangeable). Anal. Calcd. for $C_{18}H_{11}ClN_4O$: C, 64.19; H, 3.86; N, 16.64. Found: C, 64.32; H, 3.65; N, 16.40.

2-(4-Methoxyphenyl)-3-(6-oxo-1,6-dihydropyridazin-3-yl)quinoxaline (5c) was obtained as white solid, yield: 68%; mp: 200–201°C. IR (ν cm^{-1}): 3500–3300 (NH), 1680 (C=O). ^{1}H-NMR (DMSO-d_6) δ: 3.79 (s, 3H, OCH_3), 6.87-7.92 (m, 10H, 8 Ar–H and 2 pyridazinone H-4, H-5), 12.95 (s, 1H, pyridazinone NH, D_2O exchangeable). Anal. Calcd. for $C_{19}H_{14}N_4O_2$: C, 68.67; H, 4.81; N, 16.86. Found: C, 68.29; H, 5.26; N, 16.70.

6-(2-Arylethyl-1,2-dibromo)pyridazin-3(2H)-one (8a–c)

General procedure: A vigorously stirred solution of **7** (0.01 mol) in glacial acetic acid (20 ml) was heated to 70°C and then treated portionwise with bromine (0.02 mol) for 15 minutes. The mixture was stirred further for 3 hours at the same temperature and poured into ice-cold water (50 ml). The separated solid was filtered, washed with water, and crystallized from ethanol to give the dibromo derivatives **8a–c**.

6-(2-Phenylethyl-1,2-dibromo)pyridazin-3(2H)-one (8a) was obtained as a pale-yellow solid, yield: 60%; mp: 204–205°C. IR (ν, cm^{-1}): 3500–3300 (NH), 1680 (C=O); ^{1}H-NMR (DMSO-d_6) δ 5.96 (d, $J = 6$ Hz, 1H, CHBr–CHBr), 6.02 (d, $J = 6$ Hz, 1H, CHBr–CHBr), 7.04 (d, $J = 4$ Hz, 1H pyridazinone H-4), 7.34–7.66 (m, 5H, Ar–H), 7.83 (d, $J = 4$ Hz, 1H, pyridazinone H-5), 13.21 (s, 1H, pyridazinone NH, D_2O exchangeable). EIMS (*m/z*): 356 (M^+, 0.16%), 358 (M + 2, 0.29%), 360 (M + 4, 0.19%). Anal. Calcd. for $C_{12}H_{10}Br_2N_2O$: C, 40.22; H, 2.79; N, 7.82. Found: C, 40.38; H, 2.28; N, 8.27.

6-[2-(4-Chlorophenyl)ethyl-1,2-dibromo]pyridazin-3(2H)-one (8b) was obtained as a pale-yellow solid; yield: 65%; mp: 223–224°C. IR (ν, cm^{-1}): 3500–3300 (NH), 1680 (C=O); ^{1}H-NMR (DMSO-d_6) δ 5.99 (d, $J = 6$ Hz, 1H, CHBr–CHBr), 6.05 (d, $J = 6$ Hz, 1H, CHBr–CHBr), 7.02 (d, $J = 4$ Hz, 1H, pyridazinone H-4), 7.40–7.71 (dd, 4H, Ar–H), 7.9 (d, $J = 4$ Hz, 1H, pyridazinone H-5), 13.20 (s, 1H, D_2O exchangeable, NH pyridazinone). Anal. Calcd. for $C_{12}H_9Br_2ClN_2O$: C, 36.68; H, 2.29; N, 7.13. Found: C, 36.98; H, 2.59; N, 7.18.

6-[2-(4-Methoxyphenyl)ethyl-1,2-dibromo]pyridazin-3(2H)-one (8c) was obtained as a yellow solid; yield: 70%; mp: 221–222°C. IR (ν, cm^{-1}): 3500–3300 (NH), 1680 (C=O); ^{1}H-NMR (DMSO-d_6) δ: 3.82 (s, 3H, OCH_3), 5.92 (br, 1H, CHBr–CHBr), 6.14 (br, 1H, CHBr–CHBr), 6.83–8.14 (m, 6H, 4Ar–H and 2H pyridazinone H-4, H-5), 12.95 (s, 1H, D_2O exchangeable, NH pyridazinone). EIMS (*m/z*): 386 (M^+, 9.03%), 388 (M + 2, 18.11%), 390 (M + 4, 8.87%). Anal. Calcd. for $C_{13}H_{12}Br_2N_2O_2$: C, 40.20; H, 3.09; N, 7.21. Found: C, 39.85; H, 3.1; N, 7.50.

2-Aryl-3-(6-oxo-1,6-dihydropyridazin-3-yl)-1,2,3,4-tetrahydroquinoxaline (9a–c)

The appropriate dibromo derivative **8a–c** and *o*-phenylenediamine (0.001-mol each) were placed in ethanol (25 ml) along with two drops of triethylamine and the mixture was heated under reflux for 5 hours. The reaction mixture was filtered while hot, concentrated to half its volume, and poured into ice-cold water (50 ml). The separated solid was filtered, washed with water, dried, and crystallized from ethanol to give the quinoxaines **9a–c**.

2-Phenyl-3-(6-oxo-1,6-dihydropyridazin-3-yl)-1,2,3,4-tetrahydroquinoxaline (9a) was obtained as an off-white solid; yield: 75%; mp: 144–145°C. IR (ν, cm^{-1}): 3600–3300 (NH), 1660 (C=O). ^{1}H-NMR (DMSO-d_6) δ: 4.13 (d, 1H, $J = 6.4$ Hz, quinoxaline N–CH–Ar), 4.32 (d, 1H, $J = 6.4$ Hz, quinoxaline N–CH-pyridazine), 6.01 (s, 1H, quinoxaline-NH, D_2O exchangeable), 6.11 (s, 1H, D_2O exchangeable,

quinoxaline-NH), 6.47–8.20 (m, 11H, 9Ar–H and 2pyridazinone-H), 12.74 (s, 1H, NH pyridazinone, D_2O exchangeable). EIMS (*m/z*): 304 (M^+, 35.14%). Anal. Calcd. for $C_{18}H_{16}N_4O$: C, 71.05; H, 5.26; N, 18.42. Found: C, 71.37; H, 5.52; N, 18.35.

2-(4-Chlorophenyl)-3-(6-oxo-1,6-dihydropyridazin-3-yl)-1,2,3,4-tetrahydroquinoxaline (9b) was obtained as an off-white solid, yield: 76%, mp: 170–171°C. IR (ν, cm^{-1}): 3500–3300 (NH), 1660 (C=O). ^{1}H-NMR (DMSO-d_6) δ: 4.09 (d, $J = 6.4$ Hz, 1H, quinoxaline N–CH–Ar), 4.36 (d, $J = 6.4$ Hz, 1H, quinoxaline N–CH-pyridazine), 6.01 (s, 1H, quinoxaline-NH, D_2O exchangeable), 6.11 (s, 1H, quinoxaline-NH, D_2O exchangeable), 6.94–8.15 (m, 10H, 8Ar–H and 2pyridazinone-H), 12.74 (s, 1H, pyridazinone-NH, D_2O exchangeable). EIMS (*m/z*): 338 (M^+, 11.84%), 340 (M + 2, 6.54). Anal. Calcd. for $C_{18}H_{15}ClN_4O$: C, 63.81; H, 4.43; N, 16.50. Found: C, 63.56; H, 4.63; N, 16.7.

2-(4-Methoxyphenyl)-3-(6-oxo-1,6-dihydropyridazin-3-yl)-1,2,3,4-tetrahydroquinoxaline (9c) was obtained as a pale-yellow solid, yield: 76%; mp: 145–146°C. IR (ν, cm^{-1}): 3600–3300 (NH), 1660 (C=O). ^{1}H-NMR (DMSO-d_6) δ: 3.81 (s, 3H, OCH_3), 4.34 (d, 1H, $J = 6.4$ Hz, 1H, quinoxaline N–CH–Ar), 4.85 (d, 1H, $J = 6.4$ Hz, 1H, quinoxaline N–CH–Ar), 5.80 (s, 1H, quinoxaline-NH, D_2O exchangeable), 5.95 (s, 1H, quinoxaline-NH, D_2O exchangeable), 6.37–8.23 (m, 10H, 8Ar–H and 2H-pyridazinone-H), 12.76 (s, 1H, pyridazinone-NH, D_2O exchangeable). Anal. Calcd. for $C_{19}H_{18}N_4O_2$: C, 57.37; H, 3.18; N, 11.15. Found: C, 57.10; H, 3.22; N, 10.93.

6-(2-Aryl-1-bromo-2-phenylethenyl)pyridazin-3-(2H)-one (10a–b)

A mixture of the appropriate **8b–c** (0.001 mol) and ethylenediamine (0.06 g, 0.002 mol) was heated under reflux for 5 hours. The reaction mixture was filtered while hot and concentrated to half its volume. The solid separated after cooling was filtered, dried, and crystallized from ethanol to give **10a–b**.

6-(2-(4-Chlorophenyl)-1-bromoethyl)pyridazin-3-(2H)-one (10a) was obtained as a white solid, yield: 65%, mp: 278–280°C. IR (cm^{-1}): 3600–3300 (NH), 1680 (C=O), 1620 (C=N); ^{1}H-NMR (DMSO-d_6) δ: 3.79 (s, 1H, BrC=CH), 6.89–7.94 (m, 6H, 4Ar–H and 2-pyridazinone-H), 13.00 (s, 1H, NH-pyridazinone, D_2O exchangeable). EIMS (*m/z*): 311 (M^+, 6.53%); 313 (M + 2, 6.14%). Anal. Calcd. for $C_{12}H_8BrClN_2O$: C, 46.22; H, 2.56; N, 8.98; Found: C, 45.71; H, 3.10; N, 8.90.

6-(2-(4-Methoxyphenyl)-1-bromoethyl)pyridazin-3-(2H)-one (10b) was obtained as an off-white solid, yield 70%; mp: 218–219°C; IR(cm^{-1}): 3600–3300 (NH), 1680 (C=O), 1620 (C=N). ^{1}H-NMR ($CDCl_3$): 3.84(s, 3H, OCH_3), 4.72 (s, 1H, = CH), 6.80–7.64 (m, 6H, 4Ar–H and 2H-pyridazinone H-4, H-5), 10.80 (s, 1H, NH-pyridazinone, D_2O exchangeable). EIMS (*m/z*): 307 (M^+, 3.62%), 309 (M + 2, 3.41%). Anal. Calcd. for $C_{13}H_{11}BrN_2O_2$: C, 50.81; H, 3.58; N, 9.12; Found: C, 50.66; H, 3.45; N 9.16.

Effect of test compounds on paw volume in carrageenan-induced rat paw edema model (in vivo measurements)

Materials and methods

Male albino rats weighing 120–150 g (Pharmacological Department, Faculty of Pharmacy, Cairo University) were used throughout the work. They were kept in the animal house under standard conditions of light and temperature with free access to food and water. The animals were randomly divided into groups of six rats each. The paw edema was induced by subplantar injection of 50 µl of 2% carrageenan solution in saline (0.9%). Diclofenac and the test compounds were dissolved in DMSO and injected subcutaneously in 5 mg/kg body weight, 1 hour before carrageenan injection. DMSO was injected to the control group. The volume of paw edema was determined by means of water plethysmometer immediately after injection of carrageenan and 1, 2, 3, and 4 hours later.

Statistical analysis of data

The percentage protection against inflammation was calculated as follows:

$Vc - Vd/Vc \times 100$, where Vc is the increase in paw volume in the absence of the test compound (control) and Vd is the increase of paw volume after injection of the test compound. Data were expressed as the mean standard error (±SEM). Data with $P < 0.05$ value were considered to be significant (Table 1).

The % inhibition of the rat paw edema 4 hours after treatment with a single dose (5 mg/kg) of the tested compounds and their activity relative to diclofenac is presented in Table 1 and Fig. 5.

References

Abouzid K, Bekhit SA (2008) Novel anti-inflammatory agents based on pyridazinone scaffold; design, synthesis and in vivo activity. Bioorg Med Chem 16:5547–5556. doi:10.1016/j.bmc.2008.04.007

Abramson SB, Greenberg JD (2008) Are NSAIDs and selective cyclo-oxygenase 2 inhibitors associated with increased risk of myocardial infarction? Nat Clin Pract Rheumatol 4:182–183. doi:10.1038/ncprheum0763

Arber N (2008) Cyclooxygenase-2 inhibitors in colorectal cancer prevention: point. Cancer Epidemiol Biomarkers Prev 17:1852–1857. doi:10.1158/1055-9965.EPI-08-0167

Baddar FG, Nosseir MH, Doss NL, Messiha NN (1972) Pyridazines. Part 1 V. Action of Grignard reagents on 6-methyl- and 4,5- dihydro-6-α-styryl-pyridazin-3(*2H*)-ones. J Chem Soc Perkin Trans I:1091–1094. doi:10.1039/p19720001091

Beswick P, Bingham S, Bountra C, Brown T, Browning K, Campbell I, Chessell I, Clayton N, Collins S, Corfield J, Guntrip S, Haslam C, Lambeth P, Lucas F, Mathews N, Murkit G, Naylor A, Pegg N, Pickup E, Player H, Price H, Stevens A, Stratton S, Wiseman J (2004) Identification of 2,3-diaryl-pyrazolo[1,5-b]pyridazines as potent and selective cyclooxygenase-2 inhibitors. Bioorg Med Chem Lett 14:5445–5448. doi:10.1016/j.bmcl.2004.07.089

Chen Q, Praveen Rao PN, Knaus EE (2005) Design, synthesis, and biological evaluation of N-acetyl-2-carboxybenzenesulfonamides: a novel class of cyclooxygenase-2 (COX-2) inhibitors. Bioorg Med Chem 13:2459–2468. doi:10.1016/j.bmc.2005.01.039

Chintakunta VK, Akella V, Vedula MS, Mamnoor PK, Mishra P, Casturi SR, Vangoori A, Rajagopalan R (2002) 3-*O*-Substituted benzyl pyridazinone derivatives as COX inhibitors. Eur J Med Chem 37:339–347. doi:10.1016/S0223-5234(02)01336-3

Coudert P, Couquelet J, Tronche P (1988) A New synthetic route to 4,6-diarylpyridazinones and some of their derivatives. J Heterocycl chem 25:799–802

DiRosa M, Willoughby DA (1971) Screens for anti-inflammatory drugs. J Pharm Pharmacol 23:297–300

Flower RJ (2003) The development of COX2 inhibitors. Nat Rev Drug Discov 2:179–191. doi:10.1038/nrd1034

Garg R, Kurup A, Mekapati SB, Hansch C (2003) Cyclooxygenase (COX) inhibitors: a comparative QSAR study. Chem Rev 103:703–732. doi:10.1021/cr020464a

Gierse JK, McDonald JJ, Hauser SD, Rangwala SH, Koboldt CM, Seibert K (1996) A single amino acid difference between cyclooxygenase-1 (COX-1) and -2 (COX-2) reverses the selectivity of COX-2 specific inhibitors. J Biol Chem 271:15810–15814. doi:10.1074/jbc.271.26.15810

Jankowski J, Hunt R (2008) Cyclooxygenase-2 inhibitors in colorectal cancer prevention: counterpoint. Cancer Epidemiol Biomarkers Prev 17:1858–1861. doi:10.1158/1055-9965.EPI-07-0710

Joo YH, Kim JK, Kang S-H, Noh M-S, Ha J-Y, Choi JK, Lim KM, Lee CH, Chung S (2003) 2,3-Diarylbenzopyran derivatives as a novel class of selective cyclooxygenase-2 inhibitors. Bioorg Med Chem Lett 13:413–417. doi:10.1016/S0960-894X(02)00952-6

Kalgutkar AS, Zhao Z (2001) Discovery and design of selective cyclooxygenase-2 inhibitors as non-ulcerogenic, anti-inflammatory drugs with potential utility as anti-cancer agents. Curr Drug Targets 2:79–106. doi:10.2174/1389450013348830

Kurumbail RG, Stevens AM, Gierse JK, McDonald JJ, Stegeman RA, Pak JY, Gildehaus D, Miyashiro JM, Penning TD, Seibert K, Isakson PC, Stallings WC (1996) Structural basis for selective inhibition of cyclooxygenase-2 anti-inflammatory agents. Nature 384:644–648. doi:10.1038/384644a0

Li M, Wu X, Xu X (2001) Induction of apoptosis by cyclo-oxygenase-2 inhibitor NS398 through a cytochrome c-dependent pathway in esophageal cancer cells. Int J Cancer 93:218–223. doi:10.1002/ijc.1322

Li CS, Brideau C, Chan CC, Savoie C, Claveau D, Gordon CR, Greig G, Gauthier JY, Lau CK, Riendeau D, Therien M, Wong E, Prasit P (2003) Pyridazinones as selective cyclooxygenase-2 inhibitors. Bioorg Med Chem Lett 13:597–600. doi:10.1016/S0960-894X(02)01045-4

McKellar G, Madhok R, Singh G (2008) Update on the use of analgesics versus nonsteroidal anti-inflammatory drugs in rheumatic disorders: risks and benefits. Curr Opin Rheumatol 20:239–245. doi:10.1097/BOR.0b013e3282fb03ec

Ranatunge RR, Garvey DS, Janero DR, Letts LG, Martino AM, Murty MG, Richardson SK, Young DY, Zemetseva IS (2004) Synthesis and selective cyclooxygenase-2 (COX-2) inhibitory activity of a series of novel bicyclic pyrazoles. Bioorg Med Chem 12:1357–1366. doi:10.1016/j.bmc.2004.01.012

Reddy LR, Corey EJ (2005) Facile air oxidation of the conjugate base of rofecoxib (Vioxx^{TM}), a possible contributor to chronic human toxicity. Tetrahedron Lett 46:927–929. doi:10.1016/j.tetlet.2004.12.055

Sinicrope FA, Gill S (2004) Role of cyclooxygenase-2 in colorectal cancer. Cancer Metastasis Rev 23:63–75. doi:10.1023/A:1025863029529

Sircar I, Steffen RP, Bobowski G, Burke SE, Newton RS, Weishaar RE, Bristol JA, Evans DB (1989) Cardiotonic agents. 9. Synthesis and biological evaluation of a series of (E)-4,5-dihydro-6-[2-[4-(1H-imidazol-1-yl)phenyl]ethenyl]-3(2H)-pyridazinones: a novel class of compounds with positive inotropic, antithrombotic, and vasodilatory activities for the treatment of congestive heart failure. J Med Chem 32:342–350. doi:10.1021/jm00122a011

Slater EA, Wierzbicki A, Sperl G, Thompson WJ (2001) Molecular modeling study of COX-2 inhibition by diarylheterocycles and sulindac sulfide. J Mol Struct 549:111–121

Tucker ON, Dannenberg AJ, Yang EK, Zhang F, Teng L, Daly JM, Soslow RA, Masferrer JL, Woerner BM, Koki AT, Fahey TJ (1999) Cyclooxygenase-2 expression is up-regulated in human pancreatic cancer. Cancer Res 59:987–990

Uddin J, Rao P, McDonald R, Knaus EE (2004) A new class of acyclic 2-alkyl-1, 1,2-triaryl (Z)-olefins as selective cyclooxygenase-2 inhibitors. J Med Chem 47:6108–6111. doi:10.1021/jm049523y

Whitehead AJ, Ward RA, Jones MF (2007) Efficient synthesis of the selective COX-2 inhibitor GW406381X. Tetrahedron Lett 48:911–913. doi:10.1016/j.tetlet.2006.12.045

Yamac D, Ayyildiz T, Coskun U, Akyurek N, Dursun A, Seckin S, Koybasioglu F (2008). Pathol Res Pract 204:527–536. doi:10.1016/j.prp.2008.01.002

Zaheer SH, Kacker IK, Rao NS (1956) About the condensation of levulenic acid with aromatic aldehydes. Chem Ber 89:351–354. doi:10.1002/cber.19560890226